

1 International Journal of Modern Physics B  
2 Vol. 33, No. 0 (2019) 1940032 (7 pages)  
3 © World Scientific Publishing Company  
4 DOI: 10.1142/S0217979219400320



5 **Study of residual stresses in A7N01 aluminum alloy**  
6 **with X-ray diffraction Debye ring analysis**

7 Pengfei Zhu\*, Guoqing Gou\*<sup>§</sup>, Zhaofu Li<sup>†</sup>, Minhao Zhu\*,  
8 Zhongyin Zhu\*, Chuanping Ma\* and Wei Gao<sup>‡</sup>

9 \*Key Laboratory of Advanced Technologies of Materials,  
10 Ministry of Education China, Southwest Jiaotong University,  
11 Chengdu 610031, P. R. China

12 <sup>†</sup>CRRC Qingdao Sifang Locomotive Co. Ltd.,  
13 Qingdao 266550, P. R. China

14 <sup>‡</sup>Department of Chemical and Materials Engineering,  
15 The University of Auckland, PB 92019,

16 Auckland 1142, New Zealand  
17 <sup>§</sup>gouguoqing1001@163.com

18 Accepted 27 September 2018

19 Published

20 The welding residual stress has different effects on the mechanical properties of aluminum  
21 alloy welded joints, such as size stability, fatigue strength and stress corrosion cracking.  
22 Therefore, it is very important to evaluate the welding residual stress accurately. In this  
23 paper, the residual stress of A7N01 aluminum alloy welded joints was measured by X-  
24 ray diffraction. In contrast to the traditional method, the  $\cos\alpha$  method was used in this  
25 paper, the results were compared with those obtained by the conventional  $\sin^2\psi$  method.  
26 In addition, the influence of oscillation unit on the test results of the  $\cos\alpha$  method was  
27 studied.

28 *Keywords:* Residual stress; A7N01 aluminum alloy welded joints; Debye ring;  $\cos\alpha$   
29 method.

30 **AQ: Please provide PACS numbers**



31 **1. Introduction**

32 At present, the rail transit industry in China is in the stage of rapid development.  
33 For the purpose of saving energy, reducing emissions and increasing the speed of  
34 operation, it is imperative to lighten the delivery vehicle. Due to the light weight,  
35 good tensile properties and good corrosion resistance,<sup>1</sup> aluminum alloy has become  
36 the main material of rail vehicle body.

<sup>§</sup>Corresponding author.

*P. Zhu et al.*

1 However, the thermal expansion coefficient of aluminum alloy is higher than  
2 that of other metals, and the residual stress will be larger after welding. Tensile  
3 residual stress usually results in crack initiation, stress corrosion and reduces the  
4 fatigue life of components,<sup>2</sup> therefore, the accurate measurement of residual stress  
5 can better evaluate the reliability of rail train body in service.

6 X-ray diffraction method is commonly used to measure residual stress in engi-  
7 neering practice currently. The traditional  $\sin^2\psi$  method has a history of several  
8 decades,<sup>3,4</sup> and most of the previous studies of X-ray residual stress testing were  
9 based on the  $\sin^2\psi$  method. In recent years, a new method to evaluate residual  
10 stresses is proposed, which is named as the  $\cos\alpha$  method.<sup>5</sup> The  $\cos\alpha$  diffraction  
11 method is to collect data through single exposure and calculate residual stress by  
12 Debye ring while the traditional  $\sin^2\psi$  method is to use multiple exposures to fit  
13 the diffraction data obtained at different  $\psi$  angles, and finally obtain the value of  
14 residual stress. By comparison, the test time of the  $\cos\alpha$  method is shorter and the  
15 diffraction data on Debye ring is more comprehensive.<sup>6</sup> But it is difficult to measure  
16 the welding residual stress of aluminum alloy material because of the coarse grain  
17 size and the texture.

18 In this paper, the welding residual stress of aluminum alloy was measured by the  
19  $\sin^2\psi$  method and the  $\cos\alpha$  method, respectively. In order to improve the accuracy  
20 of the  $\cos\alpha$  method, an oscillation unit was added in the measuring process and the  
21 results of the residual stress were analyzed.<sup>7</sup>

## 22 **2. Experimental Procedures**

### 23 **2.1. Samples preparation**

24 A7N01-T5 aluminum alloy plates (dimensions: 300 mm  $\times$  250 mm  $\times$  8 mm) were  
25 welded by double-pass MIG welding, as shown in Fig. 1(a). The equipment used  
26 for welding is KEMPPPI KempArc-450 pulse welding machine which is shown in  
27 Fig. 1(b), and the welding wire is ER5356. Electropolishing is required before the X-  
28 ray residual stress detection, in this paper, 8818-V3 electrolytic polishing instrument  
29 was used, as shown in Fig. 1(c).

### 30 **2.2. X-ray residual stress measurement**

31 The residual stress of the welded joints was detected by two methods: the  $\sin^2\psi$   
32 method and the  $\cos\alpha$  method.

#### 33 **2.2.1. The $\sin^2\psi$ method**

34 As shown in Fig. 2(a), with the  $\sin^2\psi$  method, the residual stress is calculated by  
the change of the angle  $\psi$ . According to the theory of elasticity, strain  $\varepsilon^{\phi\psi}$  can be

# 1st Reading

## Study of residual stresses in A7N01 aluminum alloy

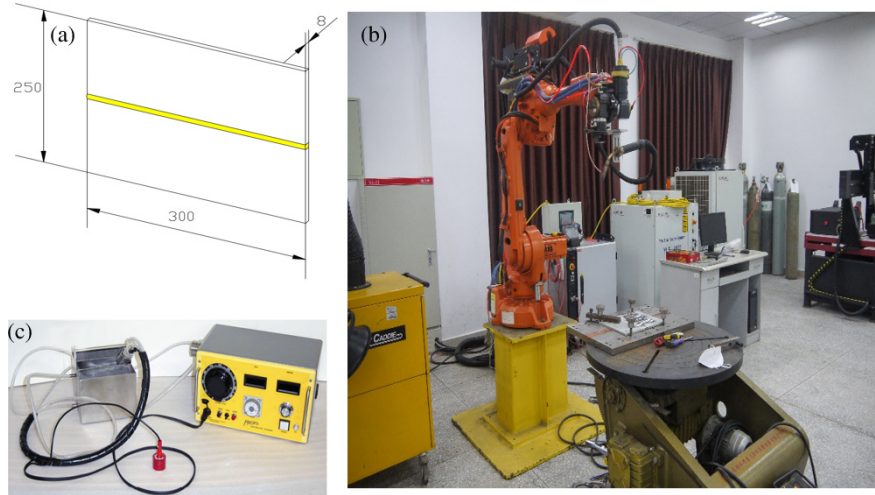


Fig. 1. (Color online) Sample preparation stage: (a) Aluminum alloy test plate size. (b) KempArc-450 pulse welding machine. (c) 8818-V3 electrolytic polishing instrument.

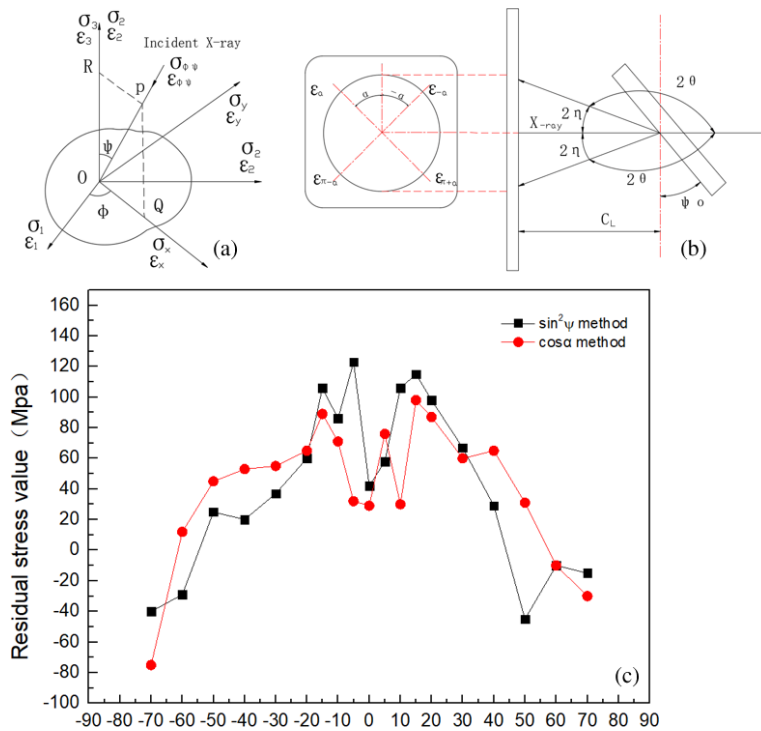


Fig. 2. (Color online) The  $\sin^2\psi$  method and the  $\cos\alpha$  method: (a) Schematic diagram of the  $\sin^2\psi$  method. (b) Schematic diagram of the  $\cos\alpha$  method; (c) Longitudinal residual stress measured by two methods.

*P. Zhu et al.*

1 expressed as

$$2 \quad \varepsilon^{\Phi\psi} = \frac{1+\nu}{E}(\sigma_x \cos^2\Phi + \tau_{xy} \sin 2\Phi + \sigma_y \sin^2\Phi - \sigma_z) \sin^2\psi \\ 3 \quad + \frac{1+\nu}{E}(\tau_{xz} \cos\Phi + \tau_{yz} \sin\Phi) \sin^2\psi + \frac{1+\nu}{E}\sigma_z - \frac{\nu}{E}(\sigma_x + \sigma_y + \sigma_z), \quad (1)$$

4 where  $\sigma_1$  and  $\sigma_2$  denote the maximum and minimum stresses in the plane, respec-  
5 tively,  $\Phi$  and  $\psi$  are the two azimuth angles of OP in any direction of space,  $\psi$  is  
6 the angle between OP and the normal line of the surface of the sample,  $\Phi$  is the  
7 angle between the projection of OP on the plane of the sample and the  $X$  axis, and  
8  $\varepsilon^{\Phi\psi}$  is the elastic strain of materials along the OP direction. In the formula,  $E$  is  
9 the elastic modulus of the material and  $\nu$  is the Poisson's ratio. This formula is the  
10 relation between macroscopic stress and strain.

11 The X-ray penetration ability is so weak that the residual stress on the surface  
12 of the material can only be measured. The stress on the surface of the material can  
13 be regarded as a two-dimensional stress, and the normal direction stress is 0. The  
14 azimuth  $\Phi$  is set to  $0^\circ$ ,  $90^\circ$  and  $45^\circ$  respectively, and the partial derivation of  $\sin^2\psi$   
15 is obtained as

$$16 \quad \sigma = K \frac{\partial 2\theta}{\partial \sin^2\psi}, \quad (2)$$

$$17 \quad K = -\frac{E}{2(1+\nu)} \cdot \cot\theta \cdot \frac{\pi}{180}, \quad (3)$$

18 where  $K$  is defined as the X-ray stress constant and  $\frac{\partial 2\theta}{\partial \sin^2\psi}$  is measured experimen-  
19 tally. This formula is the basic formula for the detection of the  $\sin^2\psi$  method.

### 20 **2.3. The $\cos\alpha$ method**

21 The residual stress will lead to the distortion of Debye ring, where the radius at  
22 different angle  $\alpha$  is not the same, as shown in Fig. 2(b). In the  $\cos\alpha$  method, the  
23 strain  $\varepsilon_\alpha$  can be used to estimate the residual stress,

$$24 \quad \varepsilon_\alpha = \frac{1}{2}[(\varepsilon_\alpha - \varepsilon_{\pi+\alpha}) + (\varepsilon_{-\alpha} - \varepsilon_{\pi-\alpha})], \quad (4)$$

$$25 \quad \sigma_x = -\frac{E}{1+\nu} \cdot \frac{1}{\sin 2\eta \sin 2\psi_0} \cdot \left( \frac{\partial \varepsilon_\alpha}{\partial \cos \alpha} \right), \quad (5)$$

26 where  $\eta$  is the mutual complementary angle of diffraction angle  $\theta$ ,  $\psi$  is the angle  
27 between the normal line of the sample surface and the angle of incidence of X-ray,  
28 and  $\sigma_x$  is the longitudinal stress.

## 29 **3. Results and Discussion**

### 30 **3.1. Residual stress measured by two methods**

31 It can be seen from Fig. 2(c) that the longitudinal stress distribution obtained with  
32 both the methods is of obvious regularity, and both show the shape of double peaks  
of residual stress distribution in aluminum alloy welding. In addition, the magnitude

*Study of residual stresses in A7N01 aluminum alloy*

1 of stress value is close to each other. The tensile stress is mostly near the center of  
 2 weld and heat affected zone, and the peak value of tensile stress is about 100 Mpa,  
 3 the stress value in the center of weld is smaller than that of the heat affected zone  
 4 on both sides of weld. In the base metal zone, the residual stress decreases with the  
 5 distance getting further from the center of the weld. The compressive stress appears  
 6 at the distance from the weld 50 mm, and the maximum compressive stress value  
 7 is about 50 Mpa.

8 By comparing the data measured by the  $\sin^2\psi$  method and the  $\cos\alpha$  method,  
 9 it can be seen that the value of residual stress in base metal position obtained by  
 10 the  $\sin^2\psi$  method is smaller than that achieved by  $\cos\alpha$  method, while the residual  
 11 stress value in heat affected zone and weld seam measured by  $\sin^2\psi$  method is larger  
 12 than that of  $\cos\alpha$  method. The trend of data measured by  $\cos\alpha$  method is more  
 13 obvious than  $\sin^2\psi$  method.

### 14 3.2. Adding the oscillation unit to the $\cos\alpha$ method

15 As shown in Fig. 3(a), the stress measuring instrument using  $\cos\alpha$  method integrates  
 16 X-ray tube and detector in a single shell. The oscillation unit is attached to the  
 17 shell of the equipment. With the oscillation of the oscillating unit, the incidence  
 18 angle of X-ray can be increased.

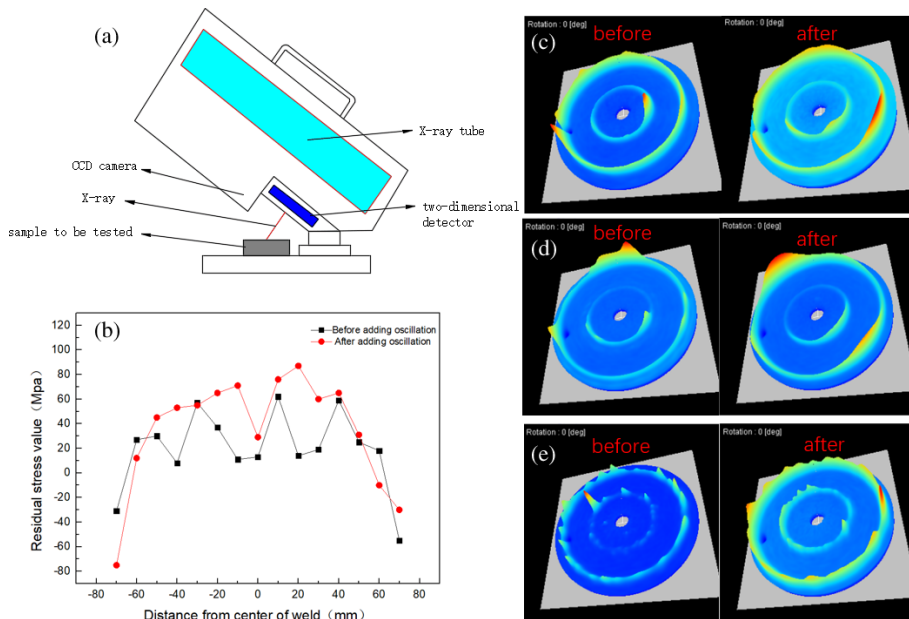


Fig. 3. (Color online) The influence of oscillation on the residual stress and Debye ring: (a) the stress measuring instrument using  $\cos\alpha$  method. (b) The residual stress before and after adding oscillation. (c) Debye ring of the base metal with oscillation and without oscillation. (d) Debye ring of the heat affected zone with oscillation and without oscillation. (e) Debye ring of the weld seam with oscillation and without oscillation.

*P. Zhu et al.*

1 The measured results of residual stress before and after adding oscillation are  
2 shown in Fig. 3(b). Compared with those without oscillation, the fluctuation of the  
3 measured results by oscillating method is obviously reduced, and shows a bimodal  
4 trend, which is consistent with the theoretical trend of welding residual stress of  
5 aluminum alloy. With the addition of oscillation, the value of residual stress in-  
6 creases slightly. There is no obvious difference of the stress values in the base metal  
7 region, and the residual stresses near the weld seam and in the heat-affected zone  
8 are quite different, which is due to the fact that less grains participate in X-ray  
9 diffraction and the numerical deviation is larger when oscillation is not added. Af-  
10 ter oscillating, the number of grains participating in diffraction increased and the  
11 measured stress values were more reliable.

12 The depth of color on the Debye ring corresponds to the intensity of the diffrac-  
13 tion peak at a certain angle, so if there is texture in the material, it will reduce  
14 the diffraction intensity of some angles, and cause the color on the Debye ring to  
15 be different in depth. In the detection of large grain samples, few number of grains  
16 involved in diffraction will lead to the absence of diffraction information at a certain  
17 angle, that is, the grain size can be estimated from the integrity of Debye ring.

18 Figure 3(c) shows Debye rings of the base metal with and without oscillation. By  
19 comparing the continuity of the two, it can be found that the shape of the Debye ring  
20 is more complete after the addition of oscillation, and there is not much difference in  
21 the overall diffraction intensity between them. Figure 3(d) shows Debye rings of the  
22 heat affected zone with and without oscillation. It can be seen that the continuity  
23 of the Debye ring detected without oscillation is poor and the diffraction intensity  
24 is low. After adding the oscillation, the integrity and strength are better than that  
25 without oscillation. The diffraction pattern of the weld zone is distributed in a  
26 dot shape when oscillation is not applied, and the diffraction intensity is uneven,  
27 as shown in Fig. 3(d). With the oscillation, the diffraction intensity is obviously  
28 improved and the vacancy between the intermittent points becomes a continuous  
29 figure. Besides, the diffraction intensity is strengthened to a certain extent. This  
30 shows that the grains involved in the diffraction are obviously increased.

#### 31 4. Conclusions

32 The  $\cos\alpha$  method is a new method to evaluate the residual stress through the Debye  
33 ring. In this paper, the welding residual stress of aluminum alloy was measured by  
34 both  $\sin^2\psi$  and  $\cos\alpha$  methods. It is found that residual stress achieved by both  
35 methods are consistent. Applying oscillation to the  $\cos\alpha$  method improved the  
36 accuracy of the residual stress measured in the aluminum alloy welded joints.

#### 37 Acknowledgment

38 The authors acknowledge the financial support from the National Key R&D Pro-  
39 gram (No. 2016YFB1200602-16).

*Study of residual stresses in A7N01 aluminum alloy*

1 **References**

- 2 1. A. J. Barnes *et al.*, *Mater. Sci. Forum.* **2118**, 361 (2013).
- 3 2. J. Y. Nam *et al.*, *Procedia Eng.* **10**, 2609 (2011).
- 4 3. J. Lin *et al.*, *J. Mater. Process. Technol.* **243**, 387 (2017).
- 5 4. J. S. Wang, C. C. Hsieh and H. H. Lai, *Mater. Charact.* **99**, 248 (2015).
- 6 5. M. Gelfi, E. Bontempi and R. Roberti, *Acta Mater.* **52**, 583 (2004).
- 7 6. D. Song *et al.*, *Corros. Sci.* **52**, 481 (2010).
- 8 7. O. Miyazaki and Y. Maruyama, *Powder Diffr.* **30**, 250 (2015).